Real-time quantitative polymerase chain reaction (PCR) analyses revealed an increase of HL expression in the livers of mice treated with LTβR-Ig ($P < 0.05$) (Fig. 4E), which may have contributed to the decrease in VLDLc levels observed in these mice. These data suggest that antagonism of the LT-LIGHT signaling pathway can increase HL expression and ameliorate the dyslipidemia in LDLR-deficient mice.

This study points to a complex interaction between T cells and liver cells in regulating lipoprotein homeostasis, mediated by two TNFSF ligands (LT and LIGHT) and their receptors. Our data raise the prospect that T cells and T cell–derived ligands might contribute directly to the complex regulation of lipid homeostasis. However, genes other than *HL* are also likely to be involved in the LTβR-dependent effects we have observed and will clearly be the focus of future studies. Finally, it is possible that LT-modulating agents may represent a novel therapeutic approach for the treatment of dyslipidemia.

References and Notes

1. C. K. Glass, J. L. Witztum, *Cell* **104**, 503 (2001).
2. P. Libby, *Nature* **420**, 868 (2002).
3. G. K. Hansson, *N. Engl. J. Med.* **352**, 1685 (2005).
4. W. Khovidhunkit *et al.*, *J. Lipid Res.* **45**, 1169 (2004).
5. Y. X. Fu, D. D. Chaplin, *Annu. Rev. Immunol.* **17**, 399 (1999).
6. J. L. Gommerman, J. L. Browning, *Nat. Rev. Immunol.* **3**, 642 (2003).
7. C. F. Ware, *Annu. Rev. Immunol.* **23**, 787 (2005).
8. S. A. Schreyer, C. M. Vick, R. C. LeBoeuf, *J. Biol. Chem.* **277**, 12364 (2002).
9. K. Ozaki *et al.*, *Nature* **429**, 72 (2004).
10. J. Wang *et al.*, *J. Clin. Invest.* **108**, 1771 (2001).
11. R. B. Shaikh *et al.*, *J. Immunol.* **167**, 6330 (2001).
12. R. A. Anders, S. K. Subudhi, J. Wang, K. Pfeffer, Y. X. Fu, *J. Immunol.* **175**, 1295 (2005).
13. S. Anand *et al.*, *J. Clin. Invest.* **116**, 1045 (2006).
14. See supporting material on *Science* Online.
15. S. Santamarina-Fojo, H. Gonzalez-Navarro, L. Freeman, E. Wagner, Z. Nong, *Arterioscler. Thromb. Vasc. Biol.* **24**, 1750 (2004).
16. D. Barcat *et al.*, *Atherosclerosis* **188**, 347 (2006).
17. H. L. Dichek *et al.*, *J. Lipid Res.* **42**, 201 (2001).
18. C. A. Reardon, G. S. Getz, *Curr. Opin. Lipidol.* **12**, 167 (2001).
19. C. A. Reardon, L. Blachowicz, J. Lukens, M. Nissenbaum, G. S. Getz, *Arterioscler. Thromb. Vasc. Biol.* **23**, 1449 (2003).

20. We thank C. Lo for help with figures, L. Blachowicz and J. Lukens for technical assistance with mice, and L. Chen for reagents. Supported by NIH grants AI062026, CA097296, and DK58891 (Y.-X.F.) and HL 85516 (G.S.G.), Heart and Stroke Foundation of Ontario grant T5642 (Z.Y.), and American Heart Association grant 0730419Z (A.V.T). J.C.L. is part of the Medical Scientist Training Program at the University of Chicago (grant 5 T32 GM07281). Array data were deposited into Gene Expression Omnibus (accession number GSE 6903),

7 November 2006; accepted 7 March 2007
10.1126/science.1137221

Structural Basis for Substrate Delivery by Acyl Carrier Protein in the Yeast Fatty Acid Synthase

Marc Leibundgut,* Simon Jenni,* Christian Frick, Nenad Ban†

In the multifunctional fungal fatty acid synthase (FAS), the acyl carrier protein (ACP) domain shuttles reaction intermediates covalently attached to its prosthetic phosphopantetheine group between the different enzymatic centers of the reaction cycle. Here, we report the structure of the *Saccharomyces cerevisiae* FAS determined at 3.1 angstrom resolution with its ACP stalled at the active site of ketoacyl synthase. The ACP contacts the base of the reaction chamber through conserved, charge-complementary surfaces, which optimally position the ACP toward the catalytic cleft of ketoacyl synthase. The conformation of the prosthetic group suggests a switchblade mechanism for acyl chain delivery to the active site of the enzyme.

Acyl carrier protein (ACP) and related substrate shuttling domains are essential in many metabolic pathways, including fatty acid, polyketide, and nonribosomal protein biosynthesis (*1*–*3*). During fatty acid synthesis, substrates are linked via a thioester bond to the prosthetic phosphopantetheine (PPT) group of ACP. In the dissociated type II fatty acid synthase (FAS) systems of most bacteria and plants, ACP is a highly abundant, small protein, which sequentially transfers the acyl-chain intermediates between the different enzymes during the cyclic reaction (*1*). The type I FAS systems of mammals, fungi, and some bacteria comprise large, multifunctional enzymes into which ACP is integrated together with the catalytic domains (*4*–*6*). This leads to a drastically increased local concentration of ACP and of all catalytic domains and allows efficient catalysis by shuttling the reaction intermediates from one reaction center to the next (*7*, *8*).

Previous structural studies of bacterial and plant type II ACPs and related carrier domains revealed that the proteins fold into a flexible all α-helical bundle (*9*–*15*). A hydrophobic cavity formed within the helix bundle of ACP shows high structural plasticity, allowing it to accommodate thioester-bound acyl-chains of different lengths (*12*, *16*).

Limited structural information about the interactions of ACP with catalytic enzymes and the mechanism of substrate delivery is currently available (*17*). Docking models, nuclear magnetic resonance and crystallographic experiments performed in the type II FAS system indicated the importance of the ACP recognition helix α2 for enzyme binding (*18*–*21*). In the structure of the fungal $\alpha_6\beta_6$ 2.6-megadalton FAS complex from *Thermomyces lanuginosus*, we observed weak electron density in both reaction chambers, possibly representing dynamically disordered ACP domains (*22*). In an attempt to gain additional information about substrate delivery by the ACP domain, we determined the structure of yeast FAS and visualized ACP stalled at the active site of ketoacyl synthase (KS), the substrate-condensing enzyme in the complex.

The *Saccharomyces cerevisiae* FAS crystal structure was solved by molecular replacement using the *T. lanuginosus* FAS coordinates (*23*). The comparison of the two homologous FAS structures reveals only minor structural differences (Fig. 1A, figs. S6 and S7). Both atomic models comprise the full set of catalytic domains involved in the fatty acid elongation cycle with an identical organization of the catalytic sites, which are pointing toward the inside of the reaction chamber. The small structural differences between the two FASs, which crystallize in different space groups and under distinct conditions, support the model for substrate shuttling without the need for large conformational changes of the enzymatic domains in the complex during the reaction cycle (*8*, *22*). In yeast FAS, we were able to identify interpretable electron density for the ACP domains at the base of the chamber, close to the catalytic cleft of the KS domain (Fig. 1A and fig. S1). Each of the three ACPs per reaction chamber is N-terminally anchored to the chamber wall and C-terminally attached to the middle of the central wheel (Fig. 1B).

The structure of the yeast ACP domain is about twice the size (18 kD) of the free-standing bacterial ACP (Fig. 2A). Fungal ACP is all α-helical, and the four N-terminal helices superimpose well with structures of plant and bacterial homologs (*12*, *16*), thereby defining the ACP core (Fig. 2A and fig. S2) (*16*). Serine $S^{180}{}_{ACP(Sc)}$ is located in a loop between helices α7 and α8, the latter corresponding to the ACP recognition helix (Fig. 2A). This residue has previously been identified as the attachment site of PPT by genetic and biochemical experiments (*24*–*27*).

Extending from the position of serine $S^{180}{}_{ACP(Sc)}$, unbiased electron density maps

Institute of Molecular Biology and Biophysics, ETH Zurich, 8092 Zurich, Switzerland.

*These authors contributed equally to this work.
†To whom correspondence should be addressed. E-mail: ban@mol.biol.ethz.ch

show the phosphate and pantoic acid moieties of the prosthetic group reaching into the active site cleft of KS (Fig. 2B). This conformation differs considerably from the one observed in the structures of *Escherichia coli* ACP in complex with acyl substrates (Fig. 2A) (*16*). In these complexes, the PPT moieties are rotated inward, and the acyl chains are buried in a deep, hydrophobic pocket formed by the ACP core, which may represent the transport form of acyl-ACP during substrate shuttling between the different catalytic domains. Notably, an empty hydrophobic pocket is recognizable also in the yeast ACP structure in complex with KS (Fig. 3A).

The N- and C-terminal tethering points on fungal ACP are opposite the site of the prosthetic group attachment, which maximizes the distance between the thiol group of the PPT arm, where the substrates are covalently bound, and the site where the flexible linkers are attached (Fig. 2A and 3A). This organization may also prevent the flexible linkers from interfering with ACP binding to the enzymes and substrate delivery.

The KS active site is located close to the approaching PPT arm of ACP and consists of a catalytic triad involving residues $C^{1305}{}_{KS(Sc)}$, $H^{1542}{}_{KS(Sc)}$, and $H^{1583}{}_{KS(Sc)}$ (Fig. 2B). The critical role of the catalytic cysteine has been established in yeast FAS by biochemical labeling and genetic experiments (*24*, *26*, *28*). Lysine $K^{1578}{}_{KS(Sc)}$ may also contribute to catalysis, because, in bacteria, a corresponding lysine is critical for decarboxylation (*29*).

We observe two major contact areas between fungal ACP and KS: The first involves the ACP core, including the ACP recognition helix α8, which contacts residues surrounding the entrance to the active site cleft of the KS core fold (Fig. 3B and figs. S2 and S3). This contact is consistent with the experiments, which demonstrate that the bacterial ACP recognition helix is important for enzyme binding (*18*–*21*). The second is formed between the additional part of the ACP domain and the large spoke of the central wheel, which consists of KS expansion segments (Fig. 3B). Notably, both subunits in the fungal KS dimer contribute to both ACP contact areas (figs. S3 and S4). The interactions of ACP with the condensing enzyme indicate a more directed mechanism for substrate delivery, rather than incidental binding of ACP-linked substrates to the KS active site.

Strong evidence indicates a physiological role for the observed interactions: (i) If we model the remaining β-alanine and cystamine moieties of the PPT arm in a sterically reasonable manner, starting from the observed pantoic acid moiety, the 18 Å–long prosthetic group extends directly into the KS catalytic cleft and terminates next to the catalytic cysteine $C^{1305}{}_{KS(Sc)}$ (Fig. 2B). (ii) ACP has patches of positively charged surface residues that interact with complementarily charged residues near the cleft entrance and in the large spoke of the central wheel (Fig. 3C). (iii) The residues that mediate the interactions are highly conserved in both the ACP domain and the reaction chamber (fig. S4D). (iv) We also observe weak electron density for ACP at a similar position above the KS in *T. lanuginosus* FAS crystals (*22*).

Although tight and preferential binding of the ACP domain to one of the catalytic domains would interfere with efficient substrate shuttling, energetically balanced, low-affinity guiding interactions for all active sites would facilitate transfer of substrates and intermediates within the reaction chamber. It is not clear why the substrate-depleted multienzyme in the crystal has stalled at this particular stage of the reaction. One possibility is that under the crystallization conditions, which favor protein-protein interactions, ACP has a higher affinity for the KS than for other catalytic sites.

Our results suggest a model of how ACP could first bind to the surface of the reaction chamber, close to the KS active site, and then use its flexible prosthetic arm to thread the acyl chain into the deep catalytic cleft. In a switchblade-like mechanism, the PPT arm carrying the acyl chain initially buried within the hydrophobic

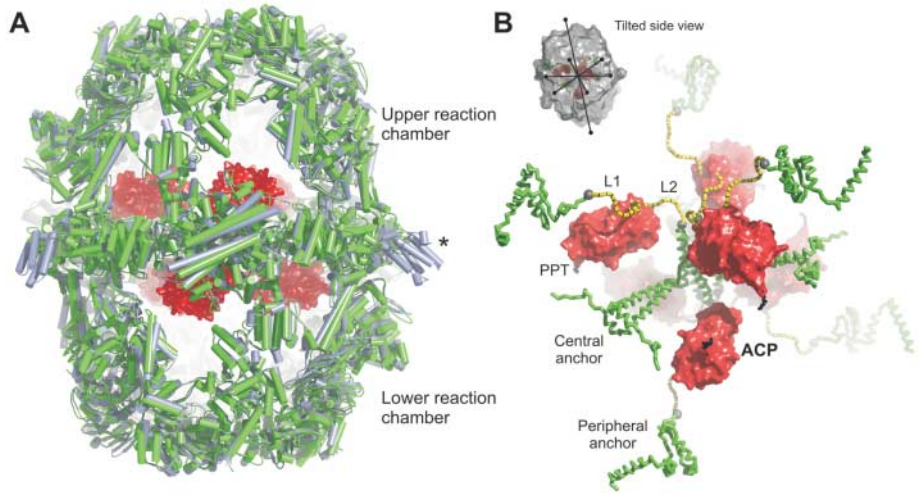

Fig. 1. Three ACPs are stalled in each of the two reaction chambers in the heterododecameric yeast FAS complex. (**A**) The superposition of the yeast (green) with the *T. lanuginosus* (light blue) FAS structure reveals a very high homology (the root mean square deviation between 19725 C_α atoms is 1.7 Å). Although ACP is disordered in the *T. lanuginosus* crystals (*22*), it is visible in yeast (red). One type of four-helix bundle at the periphery of the central wheel could only be built in *T. lanuginosus* FAS (indicated by an asterisk). (**B**) Anchoring of ACP within the reaction chambers. The ACP domains, shown as red surfaces, are located between peripheral and central anchors, which are displayed as green ribbons. The flexible linkers L1 and L2, which double-tether ACP, are not seen in the electron density map but are schematically shown as dashed yellow lines. The refined portion of the PPT prosthetic group of ACP is shown in black.

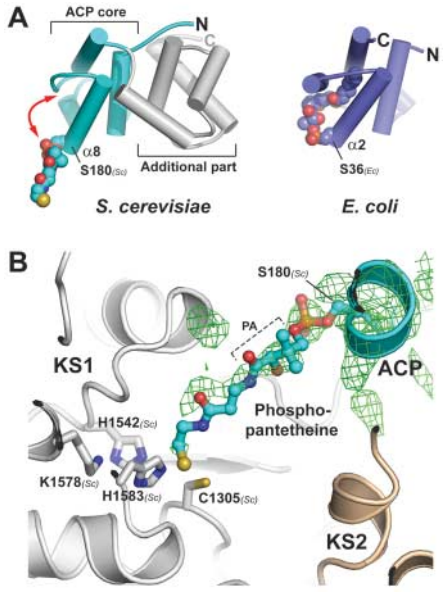

Fig. 2. Structure of yeast ACP bound to the KS catalytic cleft. (**A**) The prosthetic PPT group (spheres) covalently attached to the ACP core (cyan) adopts an extended conformation in the fungal FAS complex. The ACP core forms a compact domain with an additional four-helix bundle (gray), rendering fungal ACP considerably larger than the bacterial counterpart (blue, shown in the same orientation). During interdomain substrate shuttling, the PTT arm might fold back on ACP (arrow), thereby inserting the acyl chain into a cavity formed by the ACP core, as observed in the isolated *E. coli* ACP structure (*16*). (**B**) Detailed view of PPT bound in the catalytic cleft of KS. The unbiased threefold averaged $F_{obs} - F_{calc}$ simulated annealing omit map (green) shows ACP and the phosphate and pantoic acid (PA) moieties of the PPT prosthetic group. Modeling of the additional PPT part shows that the catalytic residues of KS can easily be reached. KS1 and KS2 form the dimer to which ACP is bound.

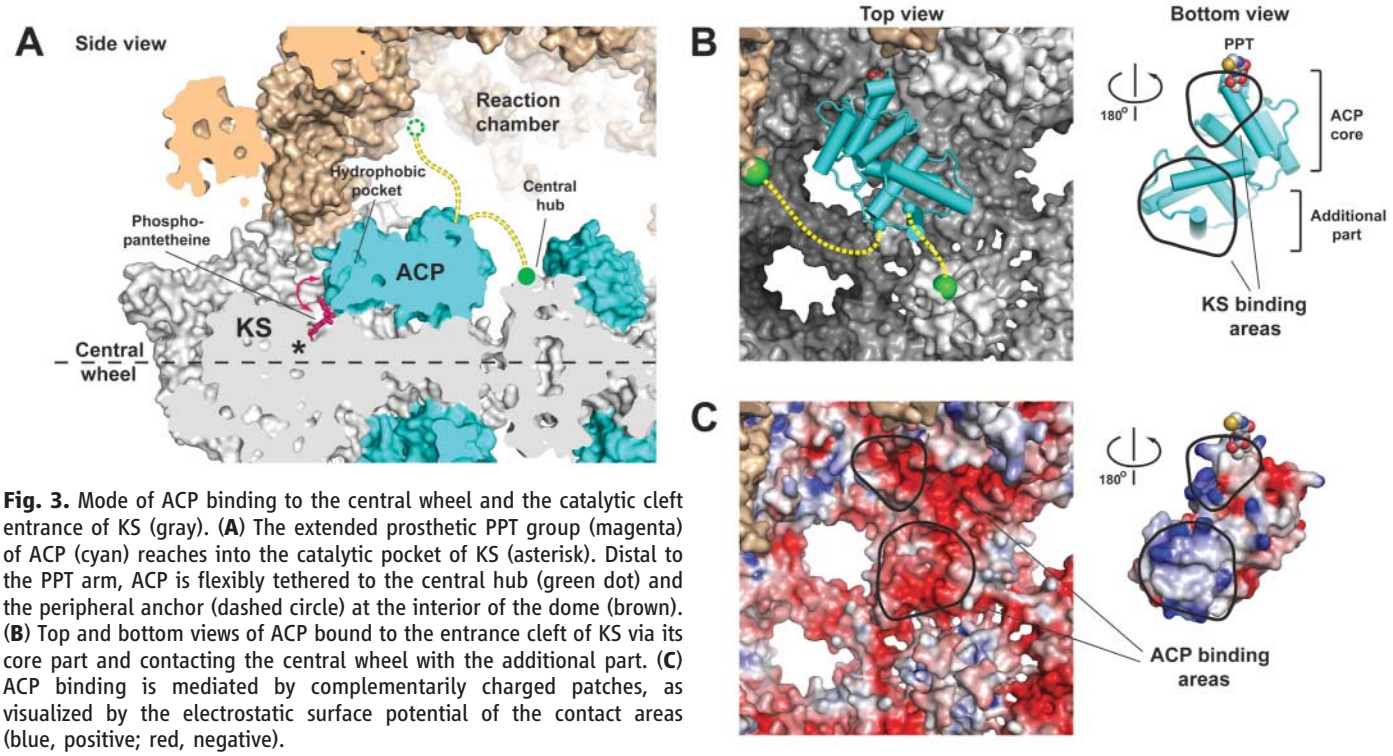

Fig. 3. Mode of ACP binding to the central wheel and the catalytic cleft entrance of KS (gray). (**A**) The extended prosthetic PPT group (magenta) of ACP (cyan) reaches into the catalytic pocket of KS (asterisk). Distal to the PPT arm, ACP is flexibly tethered to the central hub (green dot) and the peripheral anchor (dashed circle) at the interior of the dome (brown). (**B**) Top and bottom views of ACP bound to the entrance cleft of KS via its core part and contacting the central wheel with the additional part. (**C**) ACP binding is mediated by complementarily charged patches, as visualized by the electrostatic surface potential of the contact areas (blue, positive; red, negative).

ACP core would flip into the KS cleft (Fig. 3A). The binding of the ACP domain to KS might even have a more active role in the threading mechanism by stabilizing the flipped-out conformation of the loop to which the PTT arm is attached. It is noteworthy that the expansion segments of the fungal FAS structure do not merely serve as passive scaffolds for the arrangement of the catalytic domains within the complex, but also guide ACP-bound substrates to the KS. A comparable mode of action might also exist for the other catalytic domains in the FAS complex.

The assignment of the ACP domain also allows us to precisely define the amino acid sequence of the flanking linkers L1 and L2, which are flexible and not visible in the electron density (Fig. 1B). An analysis of the upstream 44–amino acid–long, alanine- and proline-rich, L1 linker sequence of fungal FAS type I ACPs reveals a striking resemblance to other carrier domain tethers, such as the biotin carboxyl carrier protein (BCCP) of the acetyl-coenzyme A carboxylase (ACC) and the lipoyl domains of the pyruvate dehydrogenase (PDH) complex in *E. coli* (fig. S5) (*30*). The fact that the linkers in the FAS complex and PDH/ACC complexes have similar composition in spite of completely different folds of the ACP and the lipoyl/BCCP domains suggests that they may have evolved convergently in fungal FAS and in the other multienzymes.

The structure of the yeast FAS complex presented here shows the direct interaction of ACP with one of the key catalytic centers in a multifunctional enzyme and suggests a model for substrate delivery that might apply to the other catalytic domains as well. These results also provide an excellent basis for future biochemical and genetic experiments in yeast, which is a well-characterized model organism.

References and Notes

1. S. W. White, J. Zheng, Y. M. Zhang, C. O. Rock, *Annu. Rev. Biochem.* **74**, 791 (2005).
2. K. J. Weissman, *Philos. Trans. A Math. Phys. Eng. Sci.* **362**, 2671 (2004).
3. R. Finking, M. A. Marahiel, *Annu. Rev. Microbiol.* **58**, 453 (2004).
4. T. Maier, S. Jenni, N. Ban, *Science* **311**, 1258 (2006).
5. S. Smith, A. Witkowski, A. K. Joshi, *Prog. Lipid Res.* **42**, 289 (2003).
6. E. Schweizer, J. Hofmann, *Microbiol. Mol. Biol. Rev.* **68**, 501 (2004).
7. F. Lynen, *Eur. J. Biochem.* **112**, 431 (1980).
8. S. Jenni, M. Leibundgut, T. Maier, N. Ban, *Science* **311**, 1263 (2006).
9. T. A. Holak, M. Nilges, J. H. Prestegard, A. M. Gronenborn, G. M. Clore, *Eur. J. Biochem.* **175**, 9 (1988).
10. G. Y. Xu *et al.*, *Structure* **9**, 277 (2001).
11. H. C. Wong, G. Liu, Y. M. Zhang, C. O. Rock, J. Zheng, *J. Biol. Chem.* **277**, 15874 (2002).
12. G. A. Zornetzer, B. G. Fox, J. L. Markley, *Biochemistry* **45**, 5217 (2006).
13. M. P. Crump *et al.*, *Biochemistry* **36**, 6000 (1997).
14. S. C. Findlow, C. Winsor, T. J. Simpson, J. Crosby, M. P. Crump, *Biochemistry* **42**, 8423 (2003).
15. A. Koglin *et al.*, *Science* **312**, 273 (2006).
16. A. Roujeinikova *et al.*, *J. Mol. Biol.* **365**, 135 (2007).
17. P. Bhaumik, M. K. Koski, T. Glumoff, J. K. Hiltunen, R. K. Wierenga, *Curr. Opin. Struct. Biol.* **15**, 621 (2005).
18. Y. M. Zhang *et al.*, *J. Biol. Chem.* **276**, 8231 (2001).
19. Y. M. Zhang, B. Wu, J. Zheng, C. O. Rock, *J. Biol. Chem.* **278**, 52935 (2003).
20. K. D. Parris *et al.*, *Structure* **8**, 883 (2000).
21. S. Rafi *et al.*, *J. Biol. Chem.* **281**, 39,285 (2006).
22. S. Jenni *et al., Science* **316**, 254 (2007).
23. Materials and methods are described in the supporting material on *Science* Online.
24. H. Schuster, B. Rautenstrauss, M. Mittag, D. Stratmann, E. Schweizer, *Eur. J. Biochem.* **228**, 417 (1995).
25. F. Fichtlscherer, C. Wellein, M. Mittag, E. Schweizer, *Eur. J. Biochem.* **267**, 2666 (2000).
26. A. H. Mohamed, S. S. Chirala, N. H. Mody, W. Y. Huang, S. J. Wakil, *J. Biol. Chem.* **263**, 12315 (1988).
27. T. Schreckenbach, H. Wobser, F. Lynen, *Eur. J. Biochem.* **80**, 13 (1977).
28. G. B. Kresze, L. Steber, D. Oesterhelt, F. Lynen, *Eur. J. Biochem.* **79**, 181 (1977).
29. P. von Wettstein-Knowles, J. G. Olsen, K. A. McGuire, A. Henriksen, *FEBS J.* **273**, 695 (2006).
30. R. N. Perham, *Annu. Rev. Biochem.* **69**, 961 (2000).

31. All data were collected at the Swiss Light Source (SLS, Paul Scherrer Institute, Villigen). We are grateful to C. Schulze-Briese, S. Gutmann, E. Pohl, S. Russo, and T. Tomizaki for their outstanding support at the SLS. We thank T. Maier and J. Erzberger for critically reading the manuscript and all members of the Ban laboratory for suggestions and discussions; R. Grosse-Kunstleve, P. Afonine, and P. Adams for providing a prerelease version of the PHENIX refinement program and advice regarding structure refinement; A. Jones for a prerelease version of the program O; D. Sargent for technical assistance. Yeast cells were kindly provided by F. Hepfer of Hefe Schweiz AG. This work was supported by the Swiss National Science Foundation (SNSF) and the National Center of Excellence in Research (NCCR) Structural Biology program of the SNSF. Coordinates and structure factors of the *S. cerevisiae* structure have been deposited in the Protein Data Bank with the accession code 2UV8.

Supporting Online Material

www.sciencemag.org/cgi/content/full/316/5822/288/DC1
Materials and Methods
Figs. S1 to S7
Tables S1 to S4
References and Notes

1 December 2006; accepted 8 March 2007
10.1126/science.1138249

Structural Basis for Substrate Delivery by Acyl Carrier Protein in the Yeast Fatty Acid Synthase

Marc Leibundgut, Simon Jenni, Christian Frick and Nenad Ban

Science **316** (5822), 288-290.
DOI: 10.1126/science.1138249